

**What do <sup>14</sup>CO  
measurements tell us  
about OH?**

M. C. Krol et al.

# What do <sup>14</sup>CO measurements tell us about OH?

**M. C. Krol<sup>1,2,3</sup>, J. Fokke Meirink<sup>2</sup>, P. Bergamaschi<sup>4</sup>, J. E. Mak<sup>5</sup>, D. Lowe<sup>6</sup>,  
P. Jöckel<sup>7</sup>, S. Houweling<sup>1,2</sup>, and T. Röckmann<sup>2</sup>**

<sup>1</sup>Netherlands Institute for Space Research (SRON), Utrecht, the Netherlands

<sup>2</sup>Institute for Marine and Atmospheric Research Utrecht (IMAU), Utrecht, the Netherlands

<sup>3</sup>Wageningen University and Research Centre (WUR), Wageningen, the Netherlands

<sup>4</sup>European Commission – DG Joint Research Centre, Institute for Environment and Sustainability, Ispra, Italy

<sup>5</sup>Institute for Terrestrial and Planetary Atmospheres, Stony Brook University, NY, USA

<sup>6</sup>National Institute of Water and Atmospheric Research, Wellington, New Zealand

<sup>7</sup>Max Planck Institute for Chemistry, Mainz, Germany

Received: 1 June 2007 – Accepted: 17 July 2007 – Published: 19 July 2007

Correspondence to: M. C. Krol (m.c.krol@phys.uu.nl)

Title Page

Abstract

Introduction

Conclusions

References

Tables

Figures

◀

▶

◀

▶

Back

Close

Full Screen / Esc

Printer-friendly Version

Interactive Discussion

## Abstract

The possible use of  $^{14}\text{CO}$  measurements to constrain hydroxyl radical (OH) concentrations in the atmosphere is investigated.  $^{14}\text{CO}$  is mainly produced in the upper atmosphere from cosmic radiation. During transport to measurement locations at the Earth's surface  $^{14}\text{CO}$  is oxidized by OH. In this paper, the sensitivity of  $^{14}\text{CO}$  mixing ratio measurements to the 3-D OH distribution is assessed with the TM5 model. Simulated  $^{14}\text{CO}$  mixing ratios compare reasonably well with atmospheric measurements taken at five locations worldwide. As a next step, the sensitivity of  $^{14}\text{CO}$  measurements to OH is calculated with the adjoint TM5 model. For our sensitivity calculations the adjoint methodology outlined in the paper offers computational advantages compared to forward model calculations. The results indicate that  $^{14}\text{CO}$  measurements, especially those taken in the tropics, are sensitive to OH in a spatially confined region. Moreover, the OH sensitivity at a certain location varies strongly over time due to meteorological variability. On average,  $^{14}\text{CO}$  measurements are about 5 times more sensitive to OH at high latitudes than to OH in the tropics. Moreover, the measurements are sensitive to OH in the main  $^{14}\text{CO}$  source region in the upper atmosphere. It will therefore be difficult to assign model-measurement discrepancies to either the  $^{14}\text{CO}$  source uncertainty or to the OH sink. Nevertheless, the large distance between the  $^{14}\text{CO}$  source region and the measurement locations should allow the retrieval of information on OH. Specifically, the sensitivity to OH in the lower atmosphere during a relatively short time span may offer the possibility to constrain local OH. These efforts will strongly depend on the number of measurements available and on our ability to accurately model the  $^{14}\text{CO}$  transport.

## 1 Introduction

$^{14}\text{CO}$  is produced in the atmosphere by neutrons that are induced by cosmic rays. Neutrons are intercepted by nitrogen nuclei forming  $^{14}\text{C}$  via  $^{14}\text{N}(n,p)^{14}\text{C}$  (Libby, 1946).

ACPD

7, 10405–10438, 2007

## What do $^{14}\text{CO}$ measurements tell us about OH?

M. C. Krol et al.

Title Page

Abstract

Introduction

Conclusions

References

Tables

Figures

⏪

⏩

◀

▶

Back

Close

Full Screen / Esc

Printer-friendly Version

Interactive Discussion

EGU

Because of the interaction of the cosmic radiation with the Earth's magnetic field, most of the production takes place at higher latitudes in the upper troposphere and lower stratosphere (UTLS).  $^{14}\text{C}$  is rapidly oxidized to  $^{14}\text{CO}$  with a yield of about 95% (MacKay et al., 1963; Pandow et al., 1960).

Measurements indicate that the  $^{14}\text{CO}$  mixing ratio at the Earth's surface ranges from less than 5 molecules  $\text{cm}^{-3}$  (throughout the manuscript the measured and modeled  $^{14}\text{CO}$  concentrations are reported at standard temperature and pressure (STP)) in the tropics to more than 25 molecules  $\text{cm}^{-3}$  STP at high latitudes (Jöckel and Brenninkmeijer, 2002; Röckmann et al., 2002). In the UTLS region, close to the source region, mixing ratios increase up to 100 molecules  $\text{cm}^{-3}$  STP (Brenninkmeijer et al., 1995; Jöckel et al., 2002). The low mixing ratios in the troposphere are mainly caused by the action of tropospheric OH that oxidizes  $^{14}\text{CO}$  to  $^{14}\text{CO}_2$ . Measurements in the atmosphere may therefore be used to indirectly estimate the abundance of OH (Brenninkmeijer et al., 1992; Jöckel et al., 2002; Mak et al., 1992; Mak and Southon, 1998; Manning et al., 2005; Volz et al., 1981). For instance, the seasonal variation of  $^{14}\text{CO}$  at high latitudes clearly signals the oxidizing action of OH in the local summer season. The lower mixing ratios in the tropics are caused by the higher abundance of OH in the tropics, and by the larger distance from the main  $^{14}\text{CO}$  production region (Jöckel et al., 2000; Mak and Southon, 1998).

Other factors also play a role. For instance, exchange between the stratosphere and the troposphere is most intense during springtime. Consequently, more  $^{14}\text{CO}$  enriched rich air enters the troposphere during this period, mainly at extra-tropical latitudes. Therefore, in order to use  $^{14}\text{CO}$  measurements to estimate tropospheric OH mixing ratios, an accurate description of the transport from the production regions to the measurement sites is required (Jöckel et al., 2000; Jöckel et al., 2002; Mak and Southon, 1998).

Due to its very low abundance, measurements of  $^{14}\text{CO}$  require very large air samples samples (typically  $0.3\text{--}1.0\text{ m}^3$ ), elaborate laboratory processing followed by both isotope ratio and accelerator mass spectrometry. Therefore, not many long-term mea-

---

## What do $^{14}\text{CO}$ measurements tell us about OH?

M. C. Krol et al.

---

[Title Page](#)[Abstract](#)[Introduction](#)[Conclusions](#)[References](#)[Tables](#)[Figures](#)[◀](#)[▶](#)[◀](#)[▶](#)[Back](#)[Close](#)[Full Screen / Esc](#)[Printer-friendly Version](#)[Interactive Discussion](#)

surement records exist. From a 13-year long record sampled at Baring Head, New Zealand, and Scott Base, Antarctica, Manning et al. (2005) estimated short-term variations of about 10% in high-latitude Southern Hemispheric OH concentrations. Moreover, estimated OH concentrations were anomalously low after the eruption of Mt Pinatubo in 1991, and after extensive wild fires in Indonesia in 1997.

Earlier, Brenninkmeijer et al. (1992) had derived higher OH concentrations in the SH compared to the NH, based on the fact that the measured  $^{14}\text{CO}$  concentration in the NH are higher compared to the SH.  $^{14}\text{CO}$  3D-transport model studies that account for the different stratosphere-troposphere exchange in both hemispheres, however, do not support such an interhemispheric asymmetry in the OH abundance (Jöckel et al., 2002; Mak et al., 1994).

First attempts to estimate the tropospheric OH concentrations from a climatology of  $^{14}\text{CO}$  (Jöckel et al., 2002) showed that the main difficulty is to separate the  $^{14}\text{CO}$  sources and sinks: an overestimate of modeled  $^{14}\text{CO}$  can be explained by either a higher tropospheric OH concentration, or by a lower source in the UTLS region.

Past efforts to estimate tropospheric OH mostly relied upon atmospheric measurements of methyl chloroform (1,1,1 trichloro-ethane, hereafter MCF), mainly because its source is better constrained (Bousquet et al., 2005; Krol and Lelieveld, 2003; Montzka et al., 2000; Prinn et al., 2005). Due to the phase-out of MCF following the Montreal protocol and its amendments, atmospheric MCF mixing ratios are declining rapidly and have reached current values of only a few parts per trillion. This implies that MCF will lose its usefulness as a species to determine OH concentrations in the near future (Lelieveld et al., 2006). Alternatives are urgently needed and in spite of the limits mentioned above  $^{14}\text{CO}$  may be a good candidate in view of its reliable production by natural processes (Brenninkmeijer, 1993).  $^{14}\text{CO}$  was successfully used as an OH calibration gas by Mak et al. (1994), who compared 2D model results to  $^{14}\text{CO}$  measurements. It was argued that the best estimates of tropospheric OH should be higher than the values used in the model, since  $^{14}\text{CO}$  was modeled about 20% too high. Later, the new OH estimates from recalibrated MCF measurements (Prinn et al., 1995) confirmed this

---

## What do $^{14}\text{CO}$ measurements tell us about OH?

M. C. Krol et al.

---

[Title Page](#)[Abstract](#)[Introduction](#)[Conclusions](#)[References](#)[Tables](#)[Figures](#)[◀](#)[▶](#)[◀](#)[▶](#)[Back](#)[Close](#)[Full Screen / Esc](#)[Printer-friendly Version](#)[Interactive Discussion](#)

finding.

Apart from the uncertain source distribution of  $^{14}\text{CO}$ , other issues need to be studied. A single  $^{14}\text{CO}$  measurement is only sensitive to the OH concentration a few months prior to sampling, due to the short  $^{14}\text{CO}$  lifetime. Moreover, the sampled air mass has encountered a specific OH history along its trajectory from the source region to the sampling site. In contrast to longer-lived species like MCF, this means that a specific  $^{14}\text{CO}$  measurement is sensitive to OH within a relatively limited distance. Thus, information on local OH can be obtained, if the specific history of each sample in terms of atmospheric transport and OH oxidation is taken into account. Whereas this effect is in principle clear, it has never been precisely quantified.

In this paper the sensitivity of single  $^{14}\text{CO}$  samples to the OH-history will be explored. These sensitivities are calculated backward in time using the adjoint of the TM5 model. The outline of the paper is as follows. The TM5  $^{14}\text{CO}$  version will be described in Sect. 2 and the result of forward simulations are described in Sect. 3. The development of the adjoint TM5 version is discussed in Sect. 4. Section 5 presents the sensitivity of single  $^{14}\text{CO}$  (and MCF) measurements to OH as calculated with the adjoint TM5 model. We finish with a discussion and conclusions in Sect. 6.

## 2 $^{14}\text{CO}$ simulations

### 2.1 Model description

The TM5 model is a global chemistry transport model (CTM) that has the ability to zoom in over specific geographical regions (Krol et al., 2005). TM5 is an off-line model, which means that meteorological fields from a weather forecast model or a climate model are used to drive the model transport. For the current study, we employ a TM5 version without using the zoom capability and without chemistry, except for the oxidation of  $^{14}\text{CO}$  by OH. Meteorological fields are taken from the ECMWF (European Centre for Medium Range Weather Forecast) model and coarsened as described in

## What do $^{14}\text{CO}$ measurements tell us about OH?

M. C. Krol et al.

Title Page

Abstract

Introduction

Conclusions

References

Tables

Figures

◀

▶

◀

▶

Back

Close

Full Screen / Esc

Printer-friendly Version

Interactive Discussion

---

**What do  $^{14}\text{C}$  measurements tell us about OH?**M. C. Krol et al.

---

Title Page

Abstract

Introduction

Conclusions

References

Tables

Figures

◀

▶

◀

▶

Back

Close

Full Screen / Esc

Printer-friendly Version

Interactive Discussion

Krol et al. (2005). The 6-hourly forecast of the operational ECMWF model is used. The TM5 vertical layer structure comprises a sub-set of the 60 layers of the hybrid sigma-pressure system of the ECMWF model. The seasonally varying climatological OH fields constructed by Spivakovsky et al. (2000) are interpolated on a grid of  $1^\circ$  longitude and  $1^\circ$  latitude, and on 60 vertical levels. The high resolution OH field is coarsened to the TM5 resolution, which is taken as  $6^\circ$  longitude  $\times$   $4^\circ$  latitude and 25 vertical layers. Two-dimensional seasonally varying stratospheric OH fields are taken from the Mainz 2-D stratospheric model (Brühl and Crutzen, 1993). Apart from removal by OH, the small but significant dry deposition of  $^{14}\text{C}$  is taken into account. Deposition velocities are calculated online during model integration based on Ganzeveld et al. (1998).

The production of  $^{14}\text{C}$  by neutrons derived from cosmic rays is strongly modulated by the solar modulation parameter ( $\Phi$ ) (Lowe and Allan, 2002). This parameter, which is expressed in MeV, indicates the minimum amount of energy a cosmic ray particle must have to avoid being deflected by the heliospheric magnetic field during its traverse to Earth. Here we use the latitudinal and height dependent production distribution calculated by Masarik and Beer (1999). The production function was calculated for a heliospheric potential of 650 MeV (intermediate solar cycle conditions), and scaled to a global production of 1 molecule  $\text{cm}^{-2}\text{s}^{-1}$  (Jöckel et al., 2002). The modulation of the global source by the heliospheric potential is calculated according to formula (5) in Lowe and Allan (2002), which is also based on Masarik and Beer (1999). Monthly values of the heliospheric potentials are presented in Usoskin et al. (2005) and the potentials for 2005 are taken from <http://cosmicrays oulu.fi/phi/> (Usoskin, personal comm.). The  $^{14}\text{C}$  source varies considerably during a solar cycle. During a solar maximum, heliospheric shielding potentials maximize and  $^{14}\text{C}$  production minimizes. Vice versa,  $^{14}\text{C}$  production maximizes during a solar minimum. Figure 1 shows the Heliospheric potential (Usoskin et al., 2005) and the corresponding  $^{14}\text{C}$  production efficiency over the 2001–2006 period. The abrupt transition from the solar maximum to the solar minimum in 2004 is clearly visible.

To calculate the  $^{14}\text{CO}$  production we assume a  $^{14}\text{C}$  to  $^{14}\text{CO}$  conversion rate of 0.95 (MacKay et al., 1963; Pandow et al., 1960).

## 2.2 Forward $^{14}\text{CO}$ simulation results

Measurements of  $^{14}\text{CO}$  are being taken at several stations worldwide. For the past three years, biweekly samples have been collected at American Samoa Observatory (14.3° S, 170.6° W, 77 m), Westmann Islands, Iceland (63.5° N, 20.3° E, 30 m) and Mauna Loa (19.54° N, 155.6° W, 3400 m). Two other sampling stations that take regular measurements are Baring Head, New Zealand (41.4° S, 174.9° E, 85 m), and Scott Base, Antarctica (77.8° S, 166.8° E, 200 m) (Manning et al., 2005).

Figure 2 shows hourly results at these five locations from a 6-year TM5 simulation (1 January 2000–1 January 2006). Only the  $^{14}\text{CO}$  that is produced by cosmic radiation has been simulated. The first simulation year was discarded as spin-up period. All tropical stations show minimum  $^{14}\text{CO}$  concentrations in local summer, and maxima in local winter. In the tropics (Mauna Loa, Samoa) simulated minima are about 3 molecules  $^{14}\text{CO cm}^{-3}$  STP. The simulated values during wintertime are much more variable and range from 5–15 molecules  $\text{cm}^{-3}$  STP.

High latitude stations show a more regular seasonal variation with generally less short-term variability. The least variable signals are simulated for Iceland and Scott Base, with summertime minima of about 4 molecules  $\text{cm}^{-3}$  STP and maxima at the end of the winter of about 13–17 molecules  $\text{cm}^{-3}$  STP.

In local winter, a high latitude reservoir of tropospheric  $^{14}\text{CO}$  builds up due to low OH and downward transport from the production region in the UTLS (Jöckel et al., 2002; Jöckel et al., 1999; Mak and Southon, 1998). Patches of air from this polar reservoir are transported equator-ward. This results in variability in the simulated  $^{14}\text{CO}$  concentrations at sampling sites at lower latitudes in winter, such as Baring Head, Samoa, and Mauna Loa. Likewise, air masses depleted in  $^{14}\text{CO}$  originating from the subtropics sometimes reach Iceland in winter. These northward transport events show

### What do $^{14}\text{CO}$ measurements tell us about OH?

M. C. Krol et al.

Title Page

Abstract

Introduction

Conclusions

References

Tables

Figures

⏪

⏩

◀

▶

Back

Close

Full Screen / Esc

Printer-friendly Version

Interactive Discussion

up as synoptic scale downward excursions of the simulated  $^{14}\text{C}$  concentrations. Such events are not simulated for Scott Base.

The red lines and symbols in Fig. 2 represent the available measurements at the stations. For Iceland, Mauna Loa, and Samoa the measurements are still in the validation phase. For this preliminary analysis, outliers were removed by hand and a 3-point moving average was applied to the data. Data points for Baring Head and Scott Base represent samples that were collected during baseline sampling conditions (Manning et al., 2005).

Measured  $^{14}\text{C}$  concentrations differ from modeled concentrations. Modeled  $^{14}\text{C}$  values represent purely cosmogenic  $^{14}\text{C}$ , while measured  $^{14}\text{C}$  contains variable amounts of recycled  $^{14}\text{C}$  due to CO production from natural volatile organic compounds (VOCs) or direct emission from biomass burning (Bergamaschi et al., 2001; Brenninkmeijer, 1993; Mak and Southon, 1998). To generate a measurement value that is representative for the cosmogenic  $^{14}\text{C}$  only, we simulated  $^{14}\text{C}$ -free CO from direct fossil emissions and from oxidation of fossil  $\text{CH}_4$ . Fossil  $\text{CH}_4$  was assumed to be 20% (340 ppb) of the atmospheric  $\text{CH}_4$  burden (Lasey et al., 2007). The modeled fossil CO at the stations was subtracted from the measured CO concentrations (STP) and the  $^{14}\text{C}$  activity of the remaining biogenic CO was taken as 120 percent modern carbon (pmC) (Bergamaschi et al., 2001). This leads to a correction of roughly 1 molecule  $^{14}\text{C}$   $\text{cm}^{-3}$  STP for each 30 ppb of biogenic CO. Typical corrections for baseline conditions are 1–2 molecules  $^{14}\text{C}$   $\text{cm}^{-3}$  STP, with larger corrections in the Northern Hemisphere.

The comparison between the modeled and corrected  $^{14}\text{C}$  measurements in Fig. 2 shows that the TM5 model is on average predicting too low  $^{14}\text{C}$  concentrations STP at high latitudes. The blue symbols in the lower panels indicate the differences between measurements and model, which appear to be systematic in nature. The model captures the measured seasonal variations very well. The measurements at Samoa and Mauna Loa seem to confirm the enhanced wintertime variability as predicted by the model. The number of samples is too small to verify the model-predicted variability

## What do $^{14}\text{C}$ measurements tell us about OH?

M. C. Krol et al.

Title Page

Abstract

Introduction

Conclusions

References

Tables

Figures

◀

▶

◀

▶

Back

Close

Full Screen / Esc

Printer-friendly Version

Interactive Discussion

on the short timescales, however.

The assumed  $^{14}\text{C}$  source height distribution in the UTLS region is a critical factor in modeling the  $^{14}\text{CO}$  distribution (Jöckel et al., 2002). This distribution depends on the shielding potential and on the calculation method. In the current approach the distribution was calculated for one fixed shielding potential (650 MeV). The source distribution of Masarik and Beer (1999) calculates a relative large fraction of the  $^{14}\text{C}$  production in the stratosphere (62–66%, Jöckel et al., 2002). The underestimate of the model at high latitudes seems to indicate that the  $^{14}\text{C}$  source region is modeled at too high altitudes or that the source strength is underestimated. Also, the stratosphere-troposphere exchange in the model can be too weak. An alternative explanation – too high OH concentrations at high latitudes - seems less likely since the OH fields are consistent with MCF observations (Spivakovsky et al., 2000). Further analysis is beyond the scope of this paper and will be addressed in a future publication.

In general, the TM5  $^{14}\text{CO}$  simulation seems to be realistic and well suited to address the main question of this paper: What is the sensitivity of a  $^{14}\text{CO}$  measurement for the OH distribution? Before addressing this question, the adjoint TM5 model will be introduced.

### 3 The adjoint TM5 model

The development of the adjoint TM5 model was initially motivated by the wish to apply variational data-assimilation methods to the optimization of trace gas emissions (e.g.  $\text{CO}_2$ ,  $\text{CH}_4$ ) using atmospheric measurements (Bergamaschi et al., 2006). The applicability of the adjoint TM5 model is, however, not limited to source optimization. For instance, the adjoint of TM5 has been used to determine the sensitivity of atmospheric measurements to (recent) upwind emissions (Gros et al., 2004; Gros et al., 2003). This sensitivity can be expressed by  $\frac{\partial \chi(t,x)}{\partial E(t',i,j)}$  for an atmospheric concentration measurement  $\chi$  at time  $t$  and location  $x$  and sources  $E(i, j)$  that were emitted at times  $t'$  before the sampling time  $t$  ( $i$  and  $j$  represent the indices of surface grid boxes

## What do $^{14}\text{CO}$ measurements tell us about OH?

M. C. Krol et al.

Title Page

Abstract

Introduction

Conclusions

References

Tables

Figures

◀

▶

◀

▶

Back

Close

Full Screen / Esc

Printer-friendly Version

Interactive Discussion

in the model). The calculation of these sensitivities requires  $n_i \times n_j$  forward simulations in which the sources  $E(i, j)$  are perturbed one after the other. The same sensitivity matrix can be calculated with only one adjoint model simulation. To this end, the adjoint model is initiated with a pulse  $ad\chi(t)$  (with “*ad*” representing an active adjoint variable, see Appendix A) at the measurement site. After the release of the pulse, the adjoint model is integrated. The pulse  $ad\chi(t)$  generates an adjoint concentration field that spreads backward in time ( $t' < t$ ) over the model domain. The adjoint concentration field is integrated in time for all surface grid-boxes to provide the adjoint emission field  $adE(i, j)$ . Since transport is described in TM5 by linear operators, the following relation holds:

$$\frac{\partial\chi(t, x)}{\partial E(t' < t, i, j)} = \frac{adE(i, j, t' < t)}{ad\chi(t, x)} \quad (1)$$

The adjoint approach offers large computational advantages, if the sensitivity for emissions (in all model grid boxes) is required for only a limited number of observations (Houweling et al., 1999; Kaminski et al., 1999).

### 3.1 Adjoint transport

The adjoint code of the two-way nested zoom model TM5 has been constructed largely by manual coding (i.e. no automatic adjoint code generator was used). Details about the adjoint TM5 model are given in Appendix A. For the application described here, the zoom algorithm is not used and only the global model domain is active.

### 3.2 Adjoint $^{14}\text{CO}$ oxidation

The adjoint TM5 model will be used to calculate the sensitivity of a measurement at a particular station to the 3-D OH distribution  $\frac{\partial\chi(t, i', j', k')}{\partial\text{OH}(t' < t, i, j, k)}$ , stating that a measurement  $\chi$  in grid box  $(i', j', k')$  and time  $t$  depends on the 3-D OH at times before the measurement was taken ( $i, j, k$  denote the three dimensions of the model-array that contains

**What do  $^{14}\text{CO}$  measurements tell us about OH?**

M. C. Krol et al.

Title Page

Abstract

Introduction

Conclusions

References

Tables

Figures

◀

▶

◀

▶

Back

Close

Full Screen / Esc

Printer-friendly Version

Interactive Discussion

the OH distribution, which varies on a monthly timescale).

As outlined in the previous section, this sensitivity field can be calculated with only one simulation in the adjoint formulation. How should the adjoint model for  $^{14}\text{CO}$  oxidation be formulated?

5 The forward model formulation of the  $^{14}\text{CO}$  oxidation in each model grid cell by OH reads (grid box indices  $i, j, k$  are dropped):

$$^{14}\text{CO}(t + dt) = ^{14}\text{CO}(t) - k\text{OH}(t)^{14}\text{CO}(t)dt \quad (2a)$$

$$\text{OH}(t + dt) = \text{OH}(t) \quad (2b)$$

10 Here, OH denotes the OH concentration (molecules  $\text{cm}^{-3}$ ),  $k$  is the second order rate constant ( $\text{cm}^3 \text{molecules}^{-1} \text{s}^{-1}$ ) for the reaction between OH and  $^{14}\text{CO}$ , and  $dt$  (s) is the time step of the model. Both OH and  $^{14}\text{CO}$  are considered active model variables (see Appendix A) since we are interested in the sensitivity of  $^{14}\text{CO}$  to OH variations. The tangent linear formulation reads:

$$d^{14}\text{CO}(t + dt) = d^{14}\text{CO}(t) - k\text{OH}(t)d^{14}\text{CO}(t)dt - kd\text{OH}(t)^{14}\text{CO}(t)dt \quad (3a)$$

$$15 \quad d\text{OH}(t + dt) = d\text{OH}(t) \quad (3b)$$

The matrix formulation of the tangent linear model reads:

$$\begin{bmatrix} d^{14}\text{CO} \\ d\text{OH} \end{bmatrix}^{(t+dt)} = \begin{bmatrix} 1 - k\text{OH}(t)dt & -k^{14}\text{CO}(t)dt \\ 0 & 1 \end{bmatrix} \begin{bmatrix} d^{14}\text{CO} \\ d\text{OH} \end{bmatrix}^{(t)} \quad (4)$$

The adjoint code is derived by transposing the forward matrix (Giering and Kaminski, 1998):

$$20 \quad \begin{bmatrix} \text{ad}^{14}\text{CO} \\ \text{adOH} \end{bmatrix}^{(t)} = \begin{bmatrix} 1 - k\text{OH}(t)dt & 0 \\ -k^{14}\text{CO}(t)dt & 1 \end{bmatrix} \begin{bmatrix} \text{ad}^{14}\text{CO} \\ \text{adOH} \end{bmatrix}^{(t+dt)}, \quad (5)$$

**What do  $^{14}\text{CO}$  measurements tell us about OH?**

M. C. Krol et al.

Title Page

Abstract

Introduction

Conclusions

References

Tables

Figures

◀

▶

◀

▶

Back

Close

Full Screen / Esc

Printer-friendly Version

Interactive Discussion

where  $ad^{14}CO$  and  $adOH$  are adjoint model variables. The adjoint code then reads:

$$ad^{14}CO(t) = ad^{14}CO(t + dt) - kOH(t)ad^{14}CO(t + dt)dt \quad (6a)$$

$$adOH(t) = adOH(t + dt) - k^{14}CO(t)ad^{14}CO(t + dt)dt \quad (6b)$$

The  $ad^{14}CO$  variable tracks the adjoint  $^{14}CO$  field that is generated by a pulse released at a measurement station. This pulse is transported backward in time in the adjoint model and is chemically destroyed by OH, similar to  $^{14}CO$  in the forward model. The  $adOH$  field accumulates the product of the forward  $^{14}CO$  field ( $kg\ m^{-3}$ ) and the adjoint  $^{14}CO$  field ( $kg^{-1}m^3$ ), multiplied by  $kdt$  ( $molecules^{-1}cm^3$ ). The units of  $adOH$  are therefore ( $molecules^{-1}cm^3$ ). The  $adOH$  field can be integrated over arbitrary time intervals and spatial domains. In practical applications the monthly integrated  $adOH$  values can be used to optimize monthly OH fields.

Note that the forward  $^{14}CO$  field has to be available during the adjoint integration. To accomplish this, the forward  $^{14}CO$  fields are stored during the forward model integration. The sensitivity of a  $^{14}CO$  measurement to OH now follows, equivalent to Eq. (1), from:

$$\frac{\partial\chi(t)}{\partial OH(i, j, k)} = \frac{adOH(i, j, k)}{ad\chi(t)}, \quad (7)$$

which states that the adjoint OH field calculated for a unit pulse  $ad\chi(t)$  at the measurement location represents the sensitivity of a measurement at that location and time to the 3-D OH field.

The correct implementation of the adjoint version of TM5, including the  $^{14}CO$  oxidation scheme, was verified by applying the adjoint test as outlined in the Appendix.

### 3.3 Adjoint OH simulations

Adjoint simulations are initialized by the simultaneous release of  $^{14}CO$  pulses at five measurement stations (Iceland, Mauna Loa, Samoa, Baring Head, and Scott Base).

## What do $^{14}CO$ measurements tell us about OH?

M. C. Krol et al.

Title Page

Abstract

Introduction

Conclusions

References

Tables

Figures

◀

▶

◀

▶

Back

Close

Full Screen / Esc

Printer-friendly Version

Interactive Discussion

The size of the pulses is not critical in the tangent linear approach and we use equal pulses of 2.5 molecules  $^{14}\text{CO cm}^{-3}$  STP at all five stations, which are added during a three-hour period. Figure 3 depicts the 3-D adjoint OH field (adOH, see Eq. 6) that results from a release at 1 January 2006 after 20 days and after one year of integration backwards in time. Note that for clarity only values between the surface and 300 hPa are shown.

For visualization, scaling with grid-box air masses is applied to the resulting 3-D adOH field. The necessity of this air mass scaling can best be understood from Eq. (7). In the equivalent forward sensitivity calculation, the 3-D OH field would be perturbed grid-box by grid-box. A normal procedure is to add a small fixed amount dOH (e.g.  $10^4$  molecules  $\text{cm}^{-3}$ ) to the OH concentration in each grid-box and to calculate the impact  $d\chi$  of this perturbation at the measurement stations. Since the grid-boxes in the model are not of equal size, this procedure implies larger perturbations (counted in molecules OH) in large grid-boxes, simply because the amount of OH added scales with the air mass that is present in each grid box. The variation in the air masses over the grid-boxes should be taken into account when the adjoint OH field is visualized. The unit of the visualized adjoint OH field is therefore ( $\text{cm}^3 \text{molecules}^{-1} (\text{kg air})^{-1}$ ). The sign of the sensitivity is negative since lower OH leads to higher  $^{14}\text{CO}$ . A larger absolute value of the adjoint OH-field implies that less OH is needed to cause a signal at the measurement sites (i.e. that the sensitivity to OH is larger).

The most striking feature of Fig. 3 is the strongly localized character of the OH sensitivity in the tropics. Even after a one-year integration the sensitivity of the different stations in the tropics can still clearly be discerned. In fact, the tropospheric sensitivity does not spread out much further in the tropics after the initial 20 days. This behavior is strongly linked to the  $^{14}\text{CO}$  lifetime. Equations 6a and b contain the factors that control the magnitude of the adOH field. These factors are:

1. The ad $^{14}\text{CO}$  field generated by the pulses released at the measurement stations (Eq. 6b). This field is subject to removal by the reaction with OH (Eq. 6a)

---

## What do $^{14}\text{CO}$ measurements tell us about OH?

M. C. Krol et al.

---

Title Page

Abstract

Introduction

Conclusions

References

Tables

Figures

⏪

⏩

◀

▶

Back

Close

Full Screen / Esc

Printer-friendly Version

Interactive Discussion

2. The  $^{14}\text{CO}$  field from the forward model integrations (Eq. 6b)

3. The reaction rate  $k$  (Eq. 6b)

Apart from these factors, transport also plays an important role. Zonal transport at the poles leads to fast mixing due to the small circumpolar distances. As discussed above, due to higher OH in the tropics and the great distance of the tropics from the source region, the tropical  $^{14}\text{CO}$  field from the forward model integration shows smaller concentrations than at high latitudes. Higher OH also implies a faster removal of the  $\text{ad}^{14}\text{CO}$  field (Eq. 6a).

Figure 4 shows the vertically integrated  $\text{adOH}$  field, again expressed per kg air. The field is shown after 20 days of integration (left panel) and after one year of integration (right panel). Note that the yellow/red colors correspond to high sensitivity. The longer integration has mainly an impact on the  $\text{adOH}$  field at higher latitudes. But even at high latitudes the signal of the first 20 days around the measurement stations remains visible. The higher sensitivity towards the poles is again explained by the longer lifetime of the adjoint  $^{14}\text{CO}$  field (lower OH) in combination with a higher value of the  $^{14}\text{CO}$  field from the forward simulation.

The  $^{14}\text{CO}$  field from the forward simulation maximizes in the source regions around the high-latitude tropopause. Although the  $\text{ad}^{14}\text{CO}$  field generated by the pulses is rather quickly oxidized in the lower atmosphere, a part of the  $\text{ad}^{14}\text{CO}$  tracer is transported upward and will reach the  $^{14}\text{CO}$  source region. This is especially true for the high latitude winter season when the  $^{14}\text{CO}$  lifetime is long. Due to the pressure dependent rate constant between OH and  $^{14}\text{CO}$ , the lifetime of  $^{14}\text{CO}$  is rather long in the UTLS region (Jöckel et al., 2000). The lingering  $\text{ad}^{14}\text{CO}$  field, combined with the high values of the forward  $^{14}\text{CO}$  field, integrates (Eq. 6b) to high values of  $\text{adOH}$ , as shown in Fig. 5. In the tropics the sensitivity is generally much lower. The first 20 days of the integration are not considered in the plot of the zonally integrated  $\text{adOH}$  field. From Fig. 4 (left panel) it is clear that a zonal integration would put much emphasis on the Scott Base station that is located close to the South Pole.

**What do  $^{14}\text{CO}$  measurements tell us about OH?**

M. C. Krol et al.

Title Page

Abstract

Introduction

Conclusions

References

Tables

Figures

◀

▶

◀

▶

Back

Close

Full Screen / Esc

Printer-friendly Version

Interactive Discussion

The lower panel of Fig. 5 integrates the adOH field (after one year, and now including the first 20 days) over atmospheric boxes of about equal mass. Due to these equal masses, the scaling is not longer necessary and the numbers represent  $(\text{adOH})^{-1}$  in the unit  $10^6 \text{ molecules cm}^{-3}$ . Note that these numbers have been obtained by spatial integration of adOH and subsequent inversion of the result. These numbers can be interpreted as the OH perturbations needed to cause the pulses at the measurement stations (see Eq. 7). The network of five stations is 4–6 times more sensitive to OH perturbations at high latitudes than to similar perturbations in the tropics.

Figure 6 shows the convergence of the inverse, globally integrated adOH field, in the unit  $10^6 \text{ molecules cm}^{-3}$  as a function of time. Convergence is reached when the released pulses are completely oxidized (Eq. 6b with vanishing  $\text{ad}^{14}\text{CO}$ ). The global integral clearly reflects the lifetime of  $^{14}\text{CO}$  (about 2 months). The final value of the global integral ( $-0.02 \times 10^6 \text{ molecules cm}^{-3}$  for pulses of  $2.5 \text{ molecules } ^{14}\text{CO cm}^{-3}$  STP at five stations) suggests a high sensitivity of the  $^{14}\text{CO}$  network for global OH that should allow the detection of changes in global OH. One should realize, however, that this sensitivity is mostly at higher latitudes and for a large part in the stratosphere (see Fig. 5).

Up to now, results from a single pulse released at five stations have been analyzed. However, the fate of the pulses just after release depends strongly on the meteorological situation. As an example, a period is selected (4 July 2005–8 July 2005) in which the simulated  $^{14}\text{CO}$  concentration varies strongly at the Samoa measurement location. Simulated concentrations at Samoa change from  $13.3 \text{ molecules } ^{14}\text{CO cm}^{-3}$  STP at 5 July (00:00 GMT) to  $6.9 \text{ molecules } ^{14}\text{CO cm}^{-3}$  STP at 8 July (00:00 GMT) (see Fig. 2). Figure 7 shows the calculated adjoint OH fields from two separate pulses released at Samoa at those times. The 8 July pulse is mainly sensitive to tropical OH. This could be expected from the low  $^{14}\text{CO}$  concentrations that signals a tropical air mass. In contrast, the July 5 pulse is also sensitive to high latitude OH. The high  $^{14}\text{CO}$  concentrations in the forward simulation is clearly caused by transport from the  $^{14}\text{CO}$  pool that is present at high latitudes in winter. Apparently, the sensitivity of a single

---

## What do $^{14}\text{CO}$ measurements tell us about OH?

M. C. Krol et al.

---

Title Page

Abstract

Introduction

Conclusions

References

Tables

Figures

◀

▶

◀

▶

Back

Close

Full Screen / Esc

Printer-friendly Version

Interactive Discussion

---

## What do $^{14}\text{CO}$ measurements tell us about OH?

M. C. Krol et al.

---

Title Page

Abstract

Introduction

Conclusions

References

Tables

Figures

◀

▶

◀

▶

Back

Close

Full Screen / Esc

Printer-friendly Version

Interactive Discussion

$^{14}\text{CO}$  measurement to OH depends strongly on the air mass from which the sample is taken. Figure 7 illustrates that in a tropical air mass a measurement is sensitive to OH close to the measurement location. In an air mass that originates from high latitudes, the measurement has additional sensitivity to OH at these higher latitudes. To highlight the sensitivity of  $^{14}\text{CO}$  measurements to the local OH concentration and the variability in this sensitivity, Fig. 8 shows the convergence of  $(\text{adOH})^{-1}$  for a  $^{14}\text{CO}$  pulse released at five consecutive days. The adOH field is integrated over a relatively small tropospheric box (see legend). Convergence in this lower tropospheric box is rather fast, and the corresponding sensitivity of the Samoa measurement to local OH relatively low ( $-3.7 \pm 0.8 \times 10^6$  molecules OH  $\text{cm}^{-3}$  for a pulse of 2.5 molecules  $^{14}\text{CO}$   $\text{cm}^{-3}$  STP). The OH sensitivity shows a high variability that is linked to – but is not entirely determined by – the forward  $^{14}\text{CO}$  mixing ratio at Samoa at the time the pulse is released.

The sensitivity of a  $^{14}\text{CO}$  measurement also depends on the season in which a sample is taken (not shown). During the high latitude winter season, released pulses survive oxidation for longer periods, which implies that the adjoint  $^{14}\text{CO}$  field contributes to the adOH integration longer.

Finally, we want to compare the OH sensitivity of  $^{14}\text{CO}$  measurements to the sensitivity of MCF measurements. Thus, we released MCF pulses (an arbitrary amount, since we are primarily interested in the distribution of the adOH field) instead of  $^{14}\text{CO}$  pulses at the five measurement stations. Since the lifetime of MCF is much longer than that of  $^{14}\text{CO}$  (5 years compared to two months), we assumed a well-mixed forward MCF field (of an arbitrary fixed concentration) in the integration of the adOH field. In practice,  $^{14}\text{CO}(t)$  was replaced by a constant in Eq. 6b. Moreover, the pressure dependent rate constant of the OH +  $^{14}\text{CO}$  reaction was replaced by the temperature dependent rate constant of the OH + MCF reaction. Figure 9 depicts the resulting adOH field after four years of integration. Note again that we focus here on the distribution of the sensitivity rather than on the absolute values. Compared to  $^{14}\text{CO}$ , the vertically integrated adOH field from MCF (right panel) shows a much higher sensitivity in the tropics. Moreover,

the sensitivity is more spread out, although the higher sensitivity close to the release points can still be discerned after four years of integration (but is sometimes blurred by the effects of orography). The zonally integrated adOH field (as for  $^{14}\text{CO}$ , the first 20 days are not considered in the zonal plot) shows that the sensitivity of MCF to OH is mainly controlled by the temperature dependent rate constant. An important factor here is the long lifetime of MCF compared to the atmospheric mixing time, which causes a rather well mixed adMCF field some months after the release of the pulses. As a result, the backward integration of the adOH field depends only on the spatial distribution of the rate constant  $k$  (Eq. 6b).

#### 4 Discussion and conclusions

The modeled distribution of  $^{14}\text{CO}$  in the period January 2001-January 2006 shows that tropical sites are characterized by large variability. In contrast, the high latitude sites show a very regular seasonal cycle. The observed and simulated maxima in winter and minima in summer are a clear effect of the summertime oxidation by OH. The variability at the tropical sites is explained by the formation of a high latitude pool of  $^{14}\text{CO}$  in the winter. For a mid-latitude station like Baring Head ( $41^\circ\text{S}$ ) more variability is simulated compared to a high latitude station like Scott Base ( $78^\circ\text{S}$ ).

Measurements confirm this picture. Manning et al. (2005) report that the concentration difference between Scott Base and Baring Head is generally smaller than 1 molecule  $\text{cm}^{-3}$  STP, except in October during the seasonal maximum. This is in excellent agreement with our simulations, presented in Fig. 10. This figure shows that the variability in the Scott Base – Baring Head concentration difference maximizes in September–November, i.e. the period of the largest latitudinal gradient in  $^{14}\text{CO}$ .

The wintertime variability increases towards the equator, which is confirmed by the preliminary  $^{14}\text{CO}$  measurements from Samoa and Mauna Loa, and by earlier measurements from Barbados (Mak and Southon, 1998), Alert and Spitsbergen (Röckmann et al., 2002) and from ship cruises (Manning et al., 2005). When interpreting  $^{14}\text{CO}$  mea-

### What do $^{14}\text{CO}$ measurements tell us about OH?

M. C. Krol et al.

Title Page

Abstract

Introduction

Conclusions

References

Tables

Figures

◀

▶

◀

▶

Back

Close

Full Screen / Esc

Printer-friendly Version

Interactive Discussion

surements, one should therefore be aware of the fact that a single measurement is possibly only a snapshot of a highly variable concentration field.

The main focus of this paper is on the sensitivity of single  $^{14}\text{CO}$  measurements to the 3-D OH field. Calculations with the adjoint TM5 model lead to the following conclusions:

- $^{14}\text{CO}$  concentrations, especially in the tropics, are sensitive to OH relatively close to the measurement station
- The sensitivity depends strongly on the origin of the air mass transported to the station
- $^{14}\text{CO}$  concentration measurements of the current measurement network are about 5 times more sensitive to high latitude OH than to tropical OH and show sensitivity to OH in the UTLS region at high latitudes

The high local sensitivity to tropical OH close to the measurement stations implies that a change of OH in the tropics influences the  $^{14}\text{CO}$  concentration only in a spatially confined region. In contrast, a change in OH in the  $^{14}\text{CO}$  source region will affect the  $^{14}\text{CO}$  field in a more or less uniform way. The calculations for Samoa indicate an average OH sensitivity of about  $3.5 \times 10^6$  molecules  $\text{cm}^{-3}$  for a  $2.5$  molecules  $\text{cm}^{-3}$  STP  $^{14}\text{CO}$  pulse (Fig. 8). The  $^{14}\text{CO}$  measurement accuracy is however about a factor of 5 better ( $0.5$  molecules  $\text{cm}^{-3}$  STP). This implies that tropical OH upstream of a measurement can be determined locally from a single  $^{14}\text{CO}$  measurement with a maximum achievable accuracy of about  $0.7 \times 10^6$  molecules  $\text{cm}^{-3}$ . Sensitivities at high latitudes are a factor 4–6 larger.

Whether or not it will be possible to use  $^{14}\text{CO}$  measurements to constrain OH will thus depend on our ability to accurately model the  $^{14}\text{CO}$  transport. Critical issues are not only the transport of  $^{14}\text{CO}$  from the source regions to the lower troposphere (like stratosphere-stratosphere exchange), but also the transport during the last few days prior to the sampling. Modern tracer transport models show increased capabilities to

## What do $^{14}\text{CO}$ measurements tell us about OH?

M. C. Krol et al.

Title Page

Abstract

Introduction

Conclusions

References

Tables

Figures

◀

▶

◀

▶

Back

Close

Full Screen / Esc

Printer-friendly Version

Interactive Discussion

simulate these processes accurately and consequently offer new possibilities to explore  $^{14}\text{CO}$  measurements.

The sensitivity of  $^{14}\text{CO}$  measurements to OH contrasts strongly with the sensitivity of MCF measurements. A comparison of Fig. 5 and Fig. 9 shows that an MCF measurement is much more sensitive to tropical OH. The adjoint formulation of the problem offers an explanation. The factors that control the differences are the rate constant (pressure dependent for  $^{14}\text{CO} + \text{OH}$ , temperature dependent for MCF + OH), and the lifetime (much shorter for  $^{14}\text{CO}$ ). Moreover, the high sensitivity of the  $^{14}\text{CO}$  concentration to high latitude UTLS OH is caused by the high  $^{14}\text{CO}$  concentration in the source region.

A logical next step following this study will be the exploration of the available  $^{14}\text{CO}$  measurements in a data-assimilation approach. In such a framework, both the sources and sinks of  $^{14}\text{CO}$  are optimized by minimizing the differences between measurements and model predictions. This will give a more definite answer to the question how the  $^{14}\text{CO}$  measurements constrain OH. Based on the current study it can be concluded that constraints on tropical OH will have a rather local character.

## Appendix A

### The adjoint TM5 model

The adjoint transport model TM5 accounts for the fact that TM5 allows two-way nested zooming. However, the current study does not use the zoom capability.

As described in more detail in (Krol et al., 2005), TM5 uses operator splitting with separate subroutines for x,y,z-advection, chemistry, emission, and vertical transport (convection and diffusion). This modular structure of the forward model is used to construct subroutines that are the adjoint of the forward routines. In this way, the correct coding of the various routines could be checked by dedicated testing routines.

Variables in the adjoint model are either active or inactive (Giering and Kaminski,

## What do $^{14}\text{CO}$ measurements tell us about OH?

M. C. Krol et al.

Title Page

Abstract

Introduction

Conclusions

References

Tables

Figures

◀

▶

◀

▶

Back

Close

Full Screen / Esc

Printer-friendly Version

Interactive Discussion

1998). Active variables represent those variables that are used in the calculation of the tangent linear derivatives (e.g. the adjoint concentration field (adrm) and the adjoint emissions (adE) from Sect. 3). Inactive variables must be identical in the forward and adjoint integrations. Examples are temperature, humidity, and winds. In an offline model like TM5 these inactive variables are stored in files and the adjoint model simply reads the same files as the forward model.

The adjoint code follows directly when the forward model is written in the form of matrices (Giering and Kaminski, 1998). The adjoint code follows by simply taking the transpose of these matrices. This procedure has been followed for the TM5 model.

A rigorous and general way to check the correct coding of the adjoint model uses a general property of a linear model:

$$\langle Lx, y \rangle = \langle x, L^T y \rangle \quad (\text{A1})$$

Here  $L$  denotes the tangent linear forward model and  $L^T$  the adjoint of the tangent linear model. Since the TM5 transport model (in the absence of any chemistry) is a linear model, it represents already the tangent linear model.  $x$  denotes the model state (all active variables) and  $y$  is the adjoint model state, and  $\langle \rangle$  denotes an inner product. A correct coding of the adjoint implies that the equality of Eq. (A1) holds for any state  $x$  and  $y$ . Note that Eq. (1) from the main text is just a specific case of Eq. A1 with  $x$  being zero apart from  $\partial E(t' < t, i, j)$  and  $y$  being zero except from  $\text{ad}\chi(t, x)$ . The adjoint TM5 was tested with a random choice of the forward ( $x$ ) and adjoint ( $y$ ) states. The equality of equation (A1) was verified to be correct up to  $O(10^{-14})$  for integration times of up to 1 year.

*Acknowledgements.* The calculations were facilitated by the Dutch National Computer Facility (NCF). J. F. Meirink is supported by a grant from NWO (EO-087). Part of the work is performed in the national BSik research program and the European FP6 program CarboEurope. We thank Rowena Moss and Gordon Brailsford for their skilled contribution to the  $^{14}\text{CO}$  analyses from Baring Head and Scott Base. Thanks go to the Iceland Meteorological Office (J. Thorlacius, O. Sigurdsson) and NOAA CMDL (M. Cunningham, SMO; J. Barnes, D. Nardini, MLO) for sample collection and logistical support. We thank Z. Wang and J. Ruggieri for sample processing.

10424

---

## What do $^{14}\text{CO}$ measurements tell us about OH?

M. C. Krol et al.

---

Title Page

Abstract

Introduction

Conclusions

References

Tables

Figures

◀

▶

◀

▶

Back

Close

Full Screen / Esc

Printer-friendly Version

Interactive Discussion

J. E. Mak's work is supported by NSF grant ATM-03037271. G. Usoskin is acknowledged for making available the 2005 heliospheric potentials.

## References

- 5 Bergamaschi, P., Frankenberg, C., Meirink, J. F., Krol, M., Dentener, F., Wagner, T., Platt, U., Kaplan, J. O., Körner, S., Heimann, M., Dlugokencky, E. J., and Goede, A.: Satellite cartography of atmospheric methane from SCIAMACHY onboard ENVISAT: (II) Evaluation based on inverse model simulations, *J. Geophys. Res.-Atmos.*, D02304, doi:10.1029/2006JD007268, 2006.
- 10 Bergamaschi, P., Lowe, D. C., Manning, M. R., Moss, R., Bromley, T., and Clarkson, T. S.: Transects of atmospheric CO, CH<sub>4</sub>, and their isotopic composition across the Pacific: Shipboard measurements and validation of inverse models, *J. Geophys. Res.-Atmos.*, 106, 7993–8011, 2001.
- 15 Bousquet, P., Hauglustaine, D. A., Peylin, P., Carouge, C., and Ciais, P.: Two decades of OH variability as inferred by an inversion of atmospheric transport and chemistry of methyl chloroform, *Atmos. Chem. Phys.*, 5, 2635–2656, 2005, <http://www.atmos-chem-phys.net/5/2635/2005/>.
- Brenninkmeijer, C. A. M.: Measurement of the Abundance of (CO)-C-14 in the Atmosphere and the C-13 C-12 and O-18 O-16 Ratio of Atmospheric CO with Applications in New-Zealand and Antarctica, *J. Geophys. Res.-Atmos.*, 98, 10595–10614, 1993.
- 20 Brenninkmeijer, C. A. M., Lowe, D. C., Manning, M. R., Sparks, R. J., and Velthoven, P. F. J. v.: The C-13, C-14 and O-18 isotopic composition of CO, CH<sub>4</sub>, and CO<sub>2</sub> in the higher southern latitudes lower stratosphere, *J. Geophys. Res.-Atmos.*, 100, 26163–26172, 1995.
- Brenninkmeijer, C. A. M., Manning, M. R., Lowe, D. C., Wallace, G., Sparks, R. J., and VolzThomas, A.: Interhemispheric Asymmetry in OH Abundance Inferred from Measurements of Atmospheric (CO)-C-14, *Nature*, 356, 50–52, 1992.
- 25 Brühl, C. and Crutzen, P. J.: The MPIC 2D model, *NASA Ref. Publ.*, 1292, 103–104, 1993.
- Ganzeveld, L., Lelieveld, J., and Roelofs, G. J.: A dry deposition parameterization for sulfur oxides in a chemistry and general circulation model, *J. Geophys. Res.-Atmos.*, 103, 5679–5694, 1998.

ACPD

7, 10405–10438, 2007

---

## What do <sup>14</sup>C measurements tell us about OH?

M. C. Krol et al.

---

Title Page

Abstract

Introduction

Conclusions

References

Tables

Figures

◀

▶

◀

▶

Back

Close

Full Screen / Esc

Printer-friendly Version

Interactive Discussion

- Giering, R. and Kaminski, T.: Recipes for adjoint code construction, *AcM Transactions on Mathematical Software*, 24, 437–474, 1998.
- Gros, V., Williams, J., Lawrence, M. G., von Kuhlmann, R., van Aardenne, J., Atlas, E., Chuck, A., Edwards, D. P., Stroud, V., and Krol, M.: Tracing the origin and ages of interlaced atmospheric pollution events over the tropical Atlantic Ocean with in situ measurements, satellites, trajectories, emission inventories, and global models, *J. Geophys. Res.-Atmos.*, 109, D22306, doi:10.129/2004JD004846, 2004.
- Gros, V., Williams, J., van Aardenne, J. A., Salisbury, G., Hofmann, R., Lawrence, M. G., von Kuhlmann, R., Lelieveld, J., Krol, M., Berresheim, H., Lobert, J. M., and Atlas, E.: Origin of anthropogenic hydrocarbons and halocarbons measured in the summertime european outflow (on Crete in 2001), *Atmos. Chem. Phys.*, 3, 1223–1235, 2003, <http://www.atmos-chem-phys.net/3/1223/2003/>.
- Houweling, S., Kaminski, T., Dentener, F., Lelieveld, J., and Heimann, M.: Inverse modeling of methane sources and sinks using the adjoint of a global transport model, *J. Geophys. Res.*, 104, 26 137–26 160, 1999.
- Jöckel, P., and Brenninkmeijer, C. A. M.: The seasonal cycle of cosmogenic (CO)-C-14 at the surface level: A solar cycle adjusted, zonal-average climatology based on observations, *J. Geophys. Res.-Atmos.*, 107, 4656, doi:10.1029/2001JD001104, 2002.
- Jöckel, P., Brenninkmeijer, C. A. M., and Lawrence, M. G.: Atmospheric response time of cosmogenic (CO)-C-14 to changes in solar activity, *J. Geophys. Res.-Atmos.*, 105, 6737–6744, 2000.
- Jöckel, P., Brenninkmeijer, C. A. M., Lawrence, M. G., Jeurken, A. B. M., and van Velthoven, P. F. J.: Evaluation of stratosphere-troposphere exchange and the hydroxyl radical distribution in three-dimensional global atmospheric models using observations of cosmogenic (CO)-C-14, *J. Geophys. Res.-Atmos.*, 107, 4446, doi:10.1029/2001JD001324, 2002.
- Jöckel, P., Lawrence, M. G., and Brenninkmeijer, C. A. M.: Simulations of cosmogenic (CO)-C-14 using the three-dimensional atmospheric model MATCH: Effects of C-14 production distribution and the solar cycle, *J. Geophys. Res.-Atmos.*, 104, 11 733–11 743, 1999.
- Kaminski, T., Heimann, M., and Giering, T.: A coarse grid three dimensional global inverse model of the atmospheric transport, 1, Adjoint Model and Jacobian Matrix, *J. Geophys. Res.*, 104, 18 535–18 553, 1999.
- Krol, M., Houweling, S., Bregman, B., van den Broek, M., Segers, A., van Velthoven, P., Peters, W., Dentener, F., and Bergamaschi, P.: The two-way nested global chemistry-transport zoom

---

## What do <sup>14</sup>CO measurements tell us about OH?

M. C. Krol et al.

---

Title Page

Abstract

Introduction

Conclusions

References

Tables

Figures

◀

▶

◀

▶

Back

Close

Full Screen / Esc

Printer-friendly Version

Interactive Discussion

model TM5: algorithm and applications, *Atmos. Chem. Phys.*, 5, 417–432, 2005,  
<http://www.atmos-chem-phys.net/5/417/2005/>.

Krol, M. and Lelieveld, J.: Can the variability in tropospheric OH be deduced from measurements of 1,1,1-trichloroethane (methyl chloroform)?, *J. Geophys. Res.*, 108, ACH 16-11–ACH 16-11, 2003.

Lassey, K. R., Lowe, D. C., and Smith, A. M.: The atmospheric cycling of radiomethane and the “fossil fraction” of the methane source, *Atmos. Chem. Phys.*, 7, 2141–2149, 2007,  
<http://www.atmos-chem-phys.net/7/2141/2007/>.

Lelieveld, J., Brenninkmeijer, C. A. M., Joeckel, P., Isaksen, I. S. A., Krol, M. C., Mak, J. E., Dlugokencky, E., Montzka, S. A., Novelli, P. C., Peters, W., and Tans, P. P.: New Directions: Watching over tropospheric hydroxyl (OH), *Atmos. Environ.*, 40, 5741–5743, 2006.

Libby, W. F.: Atmospheric Helium and radiocarbon from cosmic radiation, *Phys. Rev.*, 69, 671–672, 1946.

Lowe, D. C. and Allan, W.: A simple procedure for evaluating global cosmogenic C-14 production in the atmosphere using neutron monitor data, *Radiocarbon*, 44, 149–157, 2002.

MacKay, C., Pandow, M., and Wolfgang, R.: On the chemistry of natural radiocarbon, *J. Geophys. Res.*, 68, 3929–3931, 1963.

Mak, J. E., Brenninkmeijer, C. A. M., and Manning, M. R.: Evidence for a Missing Carbon-Monoxide Sink Based on Tropospheric Measurements of (CO)-C-14, *Geophys. Res. Lett.*, 19, 1467–1470, 1992.

Mak, J. E., Brenninkmeijer, C. A. M., and Tamareisis, J.: Atmospheric (CO)-C-14 Observations and Their Use for Estimating Carbon-Monoxide Removal Rates, *J. Geophys. Res.-Atmos.*, 99, 22 915–22 922, 1994.

Mak, J. E., and Southon, J. R.: Assessment of tropical OH seasonality using atmospheric (CO)-C-14 measurements from Barbados, *Geophys. Res. Lett.*, 25, 2801–2804, 1998.

Manning, M. R., Lowe, D. C., Moss, R. C., Bodeker, G. E., and Allan, W.: Short-term variations in the oxidizing power of the atmosphere, *Nature*, 436, 1001–1004, 2005.

Masarik, J., and Beer, J.: Simulation of particle fluxes and cosmogenic nuclide production in the Earth’s atmosphere, *J. Geophys. Res.-Atmos.*, 104, 12 099–12 111, 1999.

Montzka, S. A., Spivakovsky, C. M., Butler, J. H., Elkins, J. W., Lock, L. T., and Mondeel, D. J.: New observational constraints for atmospheric hydroxyl on global and hemispheric scales, *Science*, 288, 500–503, 2000.

Pandow, M., MacKay, C., and Wolfgang, R.: The reaction of atomic carbon with oxygen: Sig-

---

**What do <sup>14</sup>C  
measurements tell us  
about OH?**

M. C. Krol et al.

---

Title Page

Abstract

Introduction

Conclusions

References

Tables

Figures

◀

▶

◀

▶

Back

Close

Full Screen / Esc

Printer-friendly Version

Interactive Discussion

- nificance for the natural carbon cycle, *J. Inorg. Nucl. Chem.*, 14, 153–158, 1960.
- Prinn, R. G., Huang, J., Weiss, R. F., Cunnold, D. M., Fraser, P. J., Simmonds, P. G., McCulloch, A., Harth, C., Reimann, S., Salameh, P., O'Doherty, S., Wang, R. H. J., Porter, L. W., Miller, B. R., and Krummel, P. B.: Evidence for variability of atmospheric hydroxyl radicals over the past quarter century, *Geophys. Res. Lett.*, 32, L07809, doi:10.1029/2004GL022228, 2005.
- Prinn, R. G., Weiss, R. F., Miller, B. R., Huang, J., Alyea, F. N., Cunnold, D. M., Fraser, P. J., Hartley, D. E., and Simmonds, P. G.: Atmospheric Trends and Lifetime of CH<sub>3</sub>CCl<sub>3</sub> and Global OH Concentrations, *Science*, 269, 187–192, 1995.
- Röckmann, T., Jöckel, P., Gros, V., Braunlich, M., Possnert, G., and Brenninkmeijer, C. A. M.: Using C-14, C-13, O-18 and O-17 isotopic variations to provide insights into the high northern latitude surface CO inventory, *Atmos. Chem. Phys.*, 2, 147–159, 2002, <http://www.atmos-chem-phys.net/2/147/2002/>.
- Spivakovsky, C. M., Logan, J. A., Montzka, S. A., Balkanski, Y. J., Foreman-Fowler, M., Jones, D. B. A., Horowitz, L. W., Fusco, A. C., Brenninkmeijer, C. A. M., Prather, M. J., Wofsy, S. C., and McElroy, M. B.: Three-dimensional climatological distribution of tropospheric OH: Update and evaluation, *J. Geophys. Res.-Atmos.*, 105, 8931–8980, 2000.
- Usoskin, I. G., Alanko-Huotari, K., Kovaltsov, G. A., and Mursula, K.: Heliospheric modulation of cosmic rays: Monthly reconstruction for 1951–2004, *J. Geophys. Res.-Space Phys.*, 110, A12108, doi:10.1029/2005JA011250, 2005.
- Volz, A., Ehhalt, D. H., and Derwent, R. G.: Seasonal and latitudinal variation of <sup>14</sup>C and the tropospheric concentration of OH radicals, *J. Geophys. Res.*, 86, 5163–5171, 1981.

---

## What do <sup>14</sup>C measurements tell us about OH?

M. C. Krol et al.

---

Title Page

Abstract

Introduction

Conclusions

References

Tables

Figures

◀

▶

◀

▶

Back

Close

Full Screen / Esc

Printer-friendly Version

Interactive Discussion

## What do $^{14}\text{CO}$ measurements tell us about OH?

M. C. Krol et al.

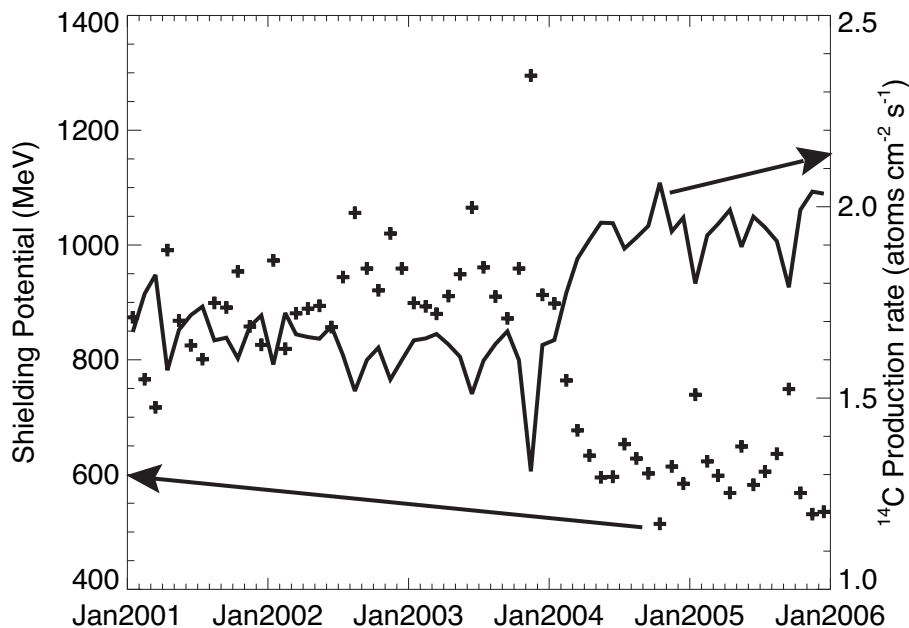


**Fig. 1.** (crosses, left axis) Monthly values of the shielding potential (Usoskin et al., 2005). (solid line, right axis)  $^{14}\text{C}$  production rate calculated from the shielding potential as described in Lowe and Allan (2002).

Title Page

Abstract

Introduction

Conclusions

References

Tables

Figures

◀

▶

◀

▶

Back

Close

Full Screen / Esc

Printer-friendly Version

Interactive Discussion

## What do $^{14}\text{CO}$ measurements tell us about OH?

M. C. Krol et al.

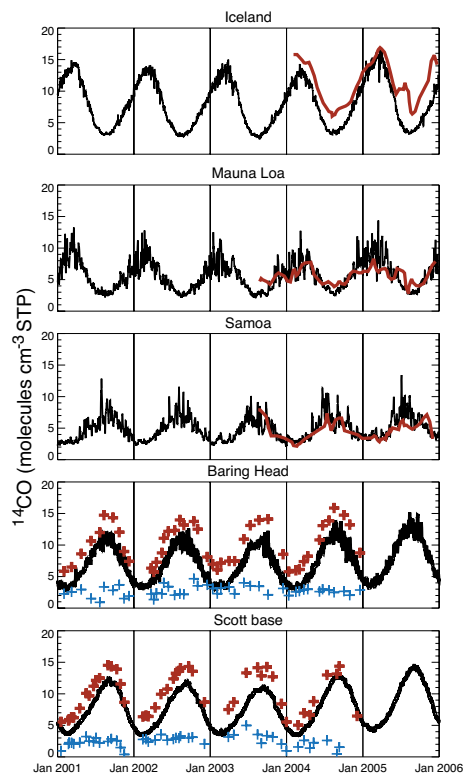


**Fig. 2.** TM5 simulated hourly cosmogenic  $^{14}\text{CO}$  concentrations (STP) at five measurement stations for Jan-2001 up to Jan-2006. For Iceland, Mauna Loa, and Samoa, a preliminary comparison to measurements that are taken about once every two weeks (red lines, 3-point smoothing applied). For Baring Head and Scott Base a comparison to individual data points is made (red crosses). The blue crosses represent the differences between measurements and model. The measurements were corrected for the recycled  $^{14}\text{CO}$  fraction.

Title Page

Abstract

Introduction

Conclusions

References

Tables

Figures

◀

▶

◀

▶

Back

Close

Full Screen / Esc

Printer-friendly Version

Interactive Discussion

---

## What do $^{14}\text{CO}$ measurements tell us about OH?

M. C. Krol et al.

---

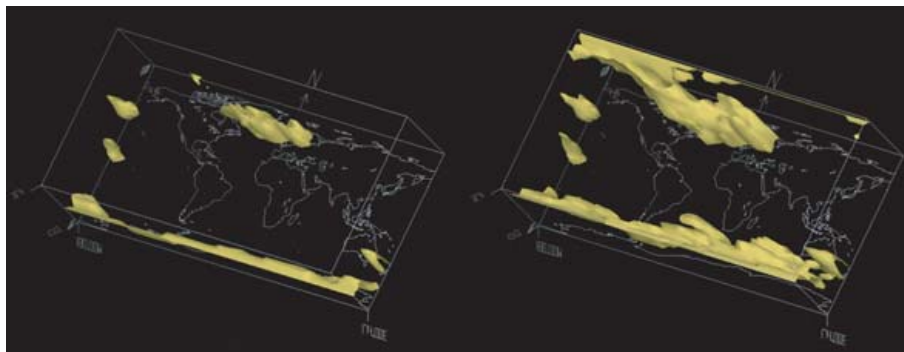


**Fig. 3.** Surface contour of the adOH field after 20 days of integration (left) and after one year of integration (right). Pulses of  $2.5 \text{ molecules } ^{14}\text{CO cm}^{-3} \text{ STP}$  were released at the five measurement stations (Iceland, Mauna Loa, Samoa, Baring Head, Scott Base). The colored contour value amounts to  $-2 \times 10^{-23} \text{ cm}^3 \text{ molecules}^{-1} (\text{kg air})^{-1}$ . The minimum value of the field amounts to  $-71 \times 10^{-23} \text{ cm}^3 \text{ molecules}^{-1} (\text{kg air})^{-1}$ . The domain runs from the surface to about 300 hPa.

[Title Page](#)[Abstract](#)[Introduction](#)[Conclusions](#)[References](#)[Tables](#)[Figures](#)[◀](#)[▶](#)[◀](#)[▶](#)[Back](#)[Close](#)[Full Screen / Esc](#)[Printer-friendly Version](#)[Interactive Discussion](#)

## What do $^{14}\text{CO}$ measurements tell us about OH?

M. C. Krol et al.

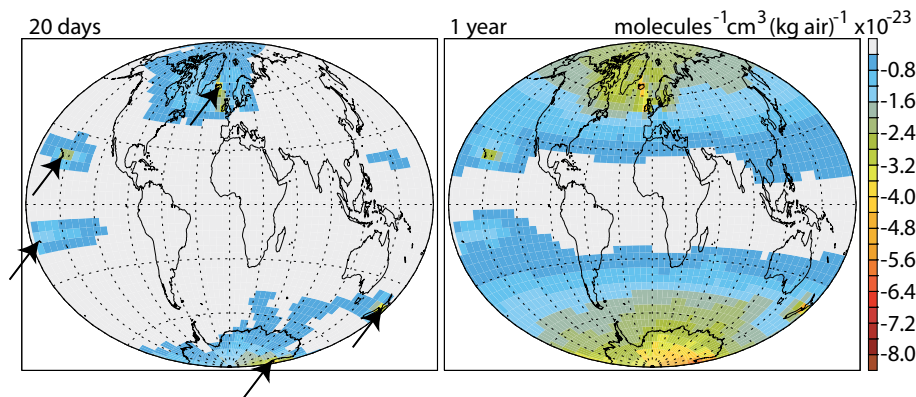


**Fig. 4.** Mass-weighted vertically integrated adOH field, see caption Fig. 3. Left: the adOH field after 20 days of integration. Right: after one year of integration. The black arrows in the leftmost panel indicate the locations where the  $^{14}\text{CO}$  pulses were released.

Title Page

Abstract

Introduction

Conclusions

References

Tables

Figures

◀

▶

◀

▶

Back

Close

Full Screen / Esc

Printer-friendly Version

Interactive Discussion

## What do $^{14}\text{CO}$ measurements tell us about OH?

M. C. Krol et al.

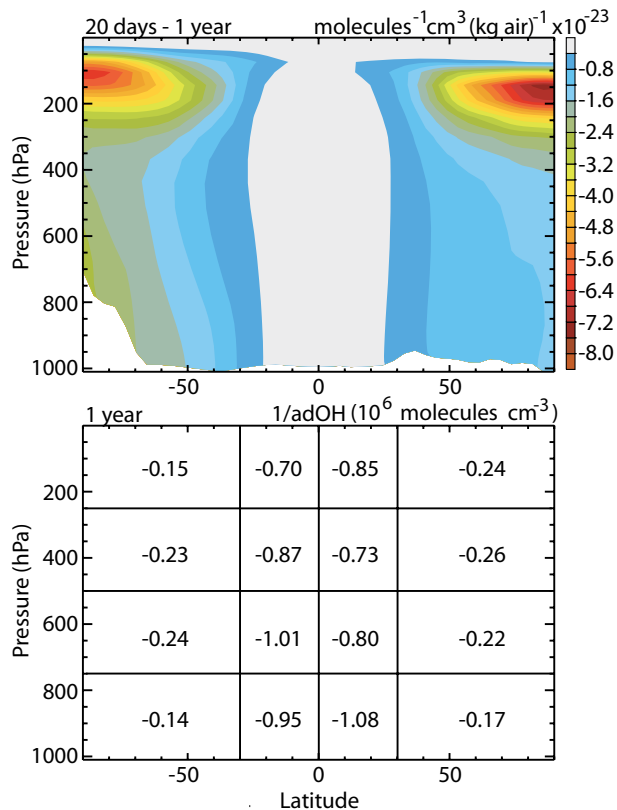


**Fig. 5.** Upper panel: Mass-weighted zonal integral of the adOH field. For clarity, the first 20 days of the adjoint integration are not considered. Lower panel: The inverse of the adOH field after one year (including the first 20 days), integrated over boxes of about equal mass in units  $10^6 \text{ molecules cm}^{-3}$ .

Title Page

Abstract

Introduction

Conclusions

References

Tables

Figures

◀

▶

◀

▶

Back

Close

Full Screen / Esc

Printer-friendly Version

Interactive Discussion

---

## What do $^{14}\text{CO}$ measurements tell us about OH?

M. C. Krol et al.

---

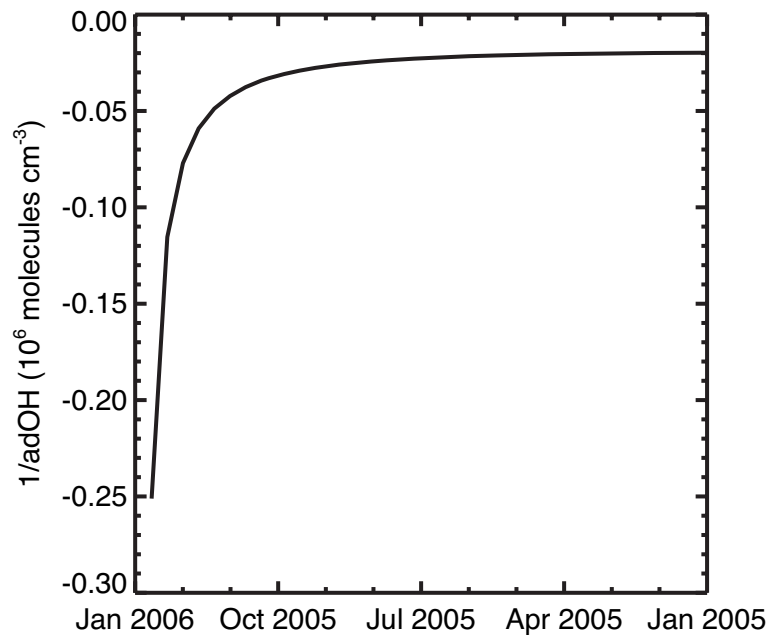


**Fig. 6.** Convergence of the adOH integration.

[Title Page](#)[Abstract](#)[Introduction](#)[Conclusions](#)[References](#)[Tables](#)[Figures](#)[◀](#)[▶](#)[◀](#)[▶](#)[Back](#)[Close](#)[Full Screen / Esc](#)[Printer-friendly Version](#)[Interactive Discussion](#)

## What do $^{14}\text{CO}$ measurements tell us about OH?

M. C. Krol et al.

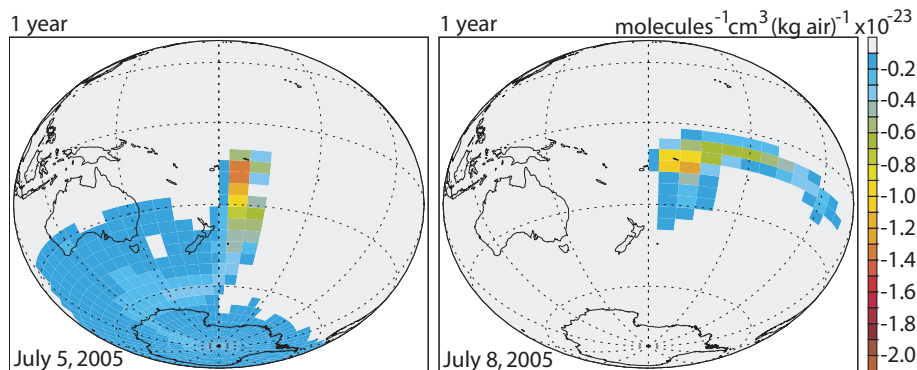


**Fig. 7.** Mass-weighted vertically integrated adOH field for a single pulse ( $2.5 \text{ molecules } ^{14}\text{CO cm}^{-3} \text{ STP}$ ) released at Samoa. Left: pulse released at 5 July 2005, 00:00 GMT. Right: pulse released at 8 July 2005, 00 GMT. The concentration in the forward simulation amount to 13.3 and 6.9  $\text{molecules } ^{14}\text{CO cm}^{-3} \text{ STP}$ , respectively.

Title Page

Abstract

Introduction

Conclusions

References

Tables

Figures

◀

▶

◀

▶

Back

Close

Full Screen / Esc

Printer-friendly Version

Interactive Discussion

## What do $^{14}\text{CO}$ measurements tell us about OH?

M. C. Krol et al.

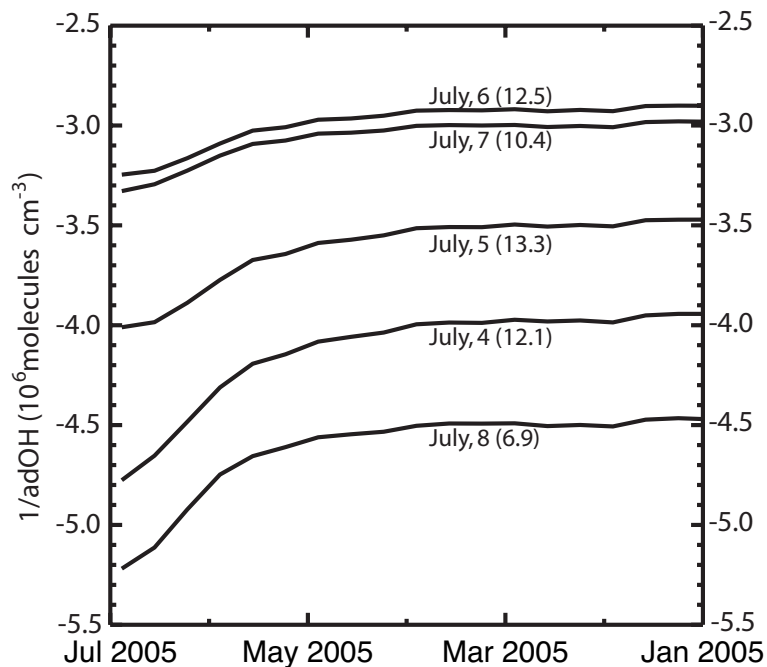


**Fig. 8.** Convergence of the  $(\text{adOH})^{-1}$  integrated over an atmospheric box around Samoa ( $180^\circ\text{E}$ – $156^\circ\text{E}$ ,  $34^\circ\text{S}$ – $6^\circ\text{S}$ , surface–500 hPa) for pulses of 2.5 molecules  $^{14}\text{CO}$   $\text{cm}^{-3}$  STP released at five consecutive days at Samoa. The values in parenthesis correspond to the simulated concentration at Samoa (molecules  $\text{cm}^{-3}$  STP).

[Title Page](#)[Abstract](#)[Introduction](#)[Conclusions](#)[References](#)[Tables](#)[Figures](#)[◀](#)[▶](#)[◀](#)[▶](#)[Back](#)[Close](#)[Full Screen / Esc](#)[Printer-friendly Version](#)[Interactive Discussion](#)

## What do $^{14}\text{CO}$ measurements tell us about OH?

M. C. Krol et al.

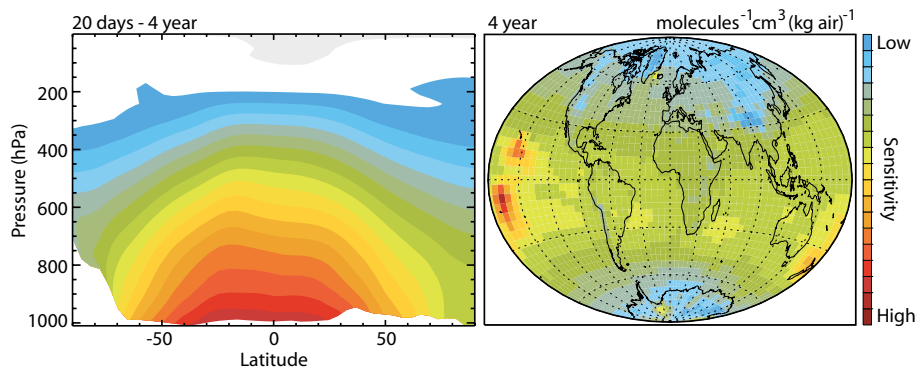


**Fig. 9.** The adOH field calculated for methyl chloroform (MCF) pulses released at the five measurement stations after 4 years integration. The required field from the forward simulation (Eq. 6b) is assumed to be well mixed. Left: Mass-weighted zonal integral, excluding the first 20 days (compare to Fig. 5). Right: Mass-weighted vertical integral (compare to Fig. 4). Only the distribution is considered important here. Red colors indicate a high sensitivity for OH (a strongly negative adOH field) and blue colors a low sensitivity.

Title Page

Abstract

Introduction

Conclusions

References

Tables

Figures

◀

▶

◀

▶

Back

Close

Full Screen / Esc

Printer-friendly Version

Interactive Discussion

## What do $^{14}\text{CO}$ measurements tell us about OH?

M. C. Krol et al.

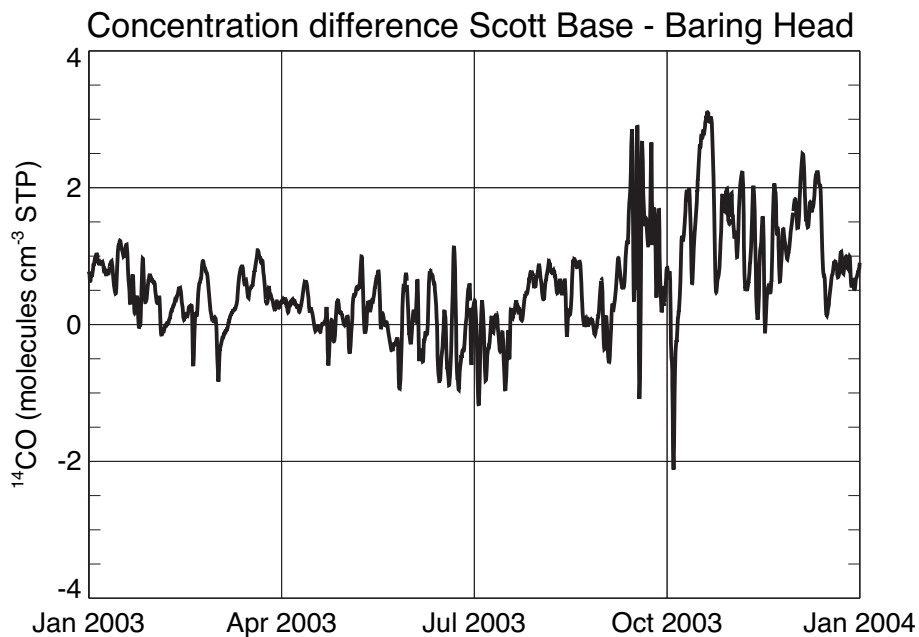


**Fig. 10.** Simulated concentration difference between Scott Base and Baring Head in 2003.

Title Page

Abstract

Introduction

Conclusions

References

Tables

Figures

◀

▶

◀

▶

Back

Close

Full Screen / Esc

Printer-friendly Version

Interactive Discussion